Chapter

Influence of Input Parameters on the Solution of Inverse Heat Conduction Problem

Rakhab C. Mehta

Abstract

A one-dimensional transient heat conduction equation is solved using analytical and numerical methods. An iterative technique is employed which estimates unknown boundary conditions from the measured temperature time history. The focus of the present chapter is to investigate effects of input parameters such as time delay, thermocouple cavity, error in the location of thermocouple position and time- and temperature-dependent thermophysical properties. Inverse heat conduction problem IHCP is solved with and without material conduction. A two-time level implicit finite difference numerical method is used to solve nonlinear heat conduction problem. Effects of uniform, nonuniform and deforming computational grids on the estimated convective heat transfer are investigated in a nozzle of solid rocket motor. A unified heat transfer analysis is presented to obtain wall heat flux and convective heat transfer coefficient in a rocket nozzle. A two-node exact solution technique is applied to estimate aerodynamic heating in a free flight of a sounding rocket. The stability of the solution of the inverse heat conduction problem is sensitive to the spatial and temporal discretization.

Keywords: analytical solution, inverse heat conduction problem, numerical analysis, deforming grid, heat transfer coefficient, heat flux, random search method

1. Introduction

The basic theory of heat and structure of solid body is associated with the internal energy of matter which in the first law of thermodynamics is referred to as the internal energy concerned with the physical state of the material. The first law of thermodynamics defines that the flowing heat energy is conserved in the absence of heat sources and sinks. It is, therefore, important to study the influence of thermocouple lead wires and distortion due to the thermocouple cavity in solution of the inverse heat conduction problem. According to the second law of thermodynamics, the heat will be transferred from one body to another body only when the bodies are at two different temperatures level and the heat will flow from the point of higher to the point of lower temperature.

A direct solution of transient heat conduction equation with prescribed initial and boundary conditions yields temperature distribution inside a slab of finite thickness. The direct solution is mathematically considered as well-posed because the solution exists, unique and continuously depends on input data. The estimation

of unknown parameters from the measured temperature history is called as inverse problem of heat conduction. It is mathematically known as an ill-posed problem since the solution now does not continuously depend on the input data. Measurement data error in temperature, thermal lagging, thermocouple's cavity, signal noise, etc. makes stability problem in the estimation of unknown parameters.

Numerical inversion of the integral solution [1], exact solution [2], numerical techniques [3], least-squares method [4], transform methods [5], different series approach [6], variable time-step size [7] have been applied to solve inverse heat conduction problems. Solutions of the ill-posed inverse heat conduction problem have been presented in detail by Beck et al. [8] and Özisik et al. [9]. Tikhonov regularization method [10] has been described for cross-validation criterion for selecting the regularization parameter to obtain a stable approximation to the solution. Kurpisz et al. [11] have presented series with derivatives with temperature to solve inverse thermal problem. Hensel [12] has described space marching numerical methods to solve inverse heat transfer problem. Various mathematical methods and numerical algorithms for solving inverse heat conduction problems are described and compared by Alifanov [13]. Taler and Duda [14] have presented solutions of direct and inverse heat conduction problems.

Inverse heat conduction analysis provides an efficient tool for estimating the thermophysical properties of materials, the boundary conditions, or the initial conditions. Estimation of surface heat flux has been carried out without [15] and with [16] heat conduction and comparison between them shows discrepancies as high as about 27% [17]. Moving window optimization method [18] has been applied to predict the aerodynamic heating in a free-flight of sounding rocket by comparing numerically calculated and measured temperature history. Howard [19] developed a numerical procedure for estimating the heat flux with variable thermal properties using a single embedded thermocouple. Simultaneous identification of the temperature-dependent thermal conductivity and the asymmetry parameter of the Henyey-Greenstein scattering phase function have been shown by Zmywaczyk and Koniorczyk [20].

The conjugate gradient method with adjoint problem for function estimation iterative technique is used to solve IHCP to estimate heat flux and internal wall temperature of the throat section of the rocket nozzle [21]. Heisler [22] have reported supplementary "short-time" temperature-time charts for the center, midlocation and surface of large plates, long cylinders and spheres for the dimensionless time sub-domain. Convective heat transfer coefficient and combustion temperature in a rocket nozzle is determined using transient-temperature response chart [23].

The solution of transient IHCP can be obtained using analytical or numerical schemes in conjunction with measured temperature-time history. The estimation of the unknown parameters can be carried out by employing gradient or non-gradient methods to predict the unknown parameters in a prescribed tolerance limit. The focus of the present work is to investigate the influence of various parameters on the solution of inverse heat conduction problem.

2. Measurement errors

Experimental difficulties [24] are noticed in implanting thermocouples at the surface for temperature measurements. Temperature response delays have been studied to solve IHCP applied to cooled rocket thrust chamber [25]. The temperature measured inside the slab may delay and damp depending on x_m as illustrated in **Figure 1**. A thermocouple indicates temperature lag behind the actual temperature. The effect of the thermocouple sensor dynamics on prediction of a triangular heat

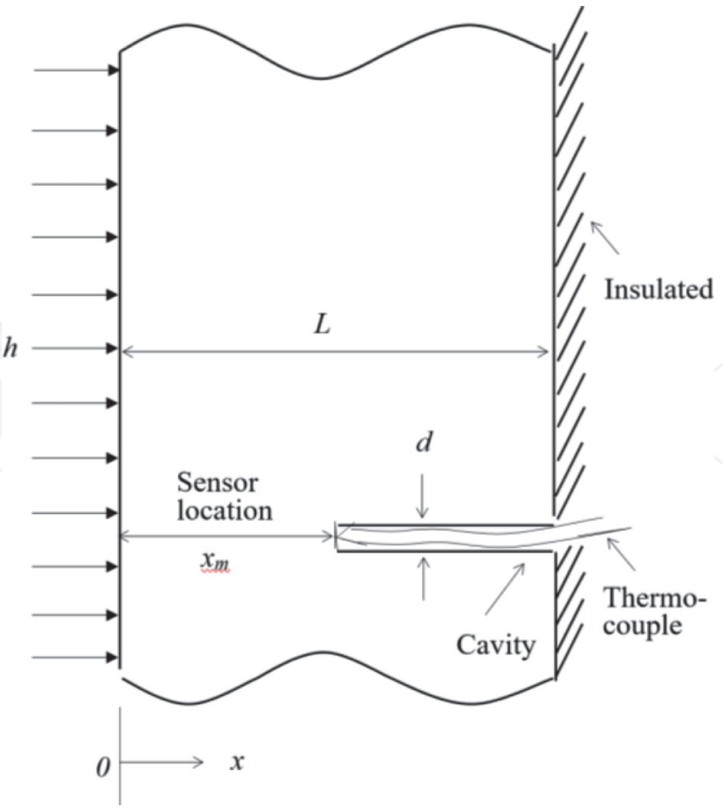

Figure 1.
Geometry of the specimen.

flux history has been analyzed with simulated data in a one-dimensional domain by Woodbury [26].

Chen and Danh [27] have carried out experimental studies to obtain transient temperature distortion and thermal delay in a slab due to presence of thermocouple cavity. The distortion of temperature profiles inside the slab may be influenced by the dissimilar thermophysical properties of thermocouple and surrounding materials and by the diameter and depth of the cavity. The temperature distortion [28] inside a slab is a function of the thermocouple cavity diameter d and location x_m.

Standard statistical analysis consists of error in the measurement as an additive of true plus random, in zero mean, in constant variance, uncorrelated, normal, bell shaped probability density function, constant variance known, errors in the dependent variables and no-prior information about the parameters. The error in measurement can be obtain using exact analytical solution [29] as

$$E = \cos(x/L)(\cos\varepsilon - 1)e^{-\delta\tau} \tag{1}$$

$$E = \sin(x/L)(\cos\varepsilon - 1)e^{-\delta\tau} \tag{2}$$

where ε and $\delta\tau$ refer to error in measurement of thermocouple location and in time recording, respectively. One of the important points that must be mentioned, here, is the use of a starting solution. In the case of a solid rocket motor where boundary conditions are suddenly imposed by a wall, there will be high intensity of heat flux on cold wall, and the heat flux during the first few steps in time may not be very accurate. The numerical solution is initiated using an exact analytical solution instead of starting from the initial constant condition. Such solutions can be obtained from to exact analytical solution [30] of transient heat conduction equation. Heat transfer rates to the calorimetric probe are estimated from measurements of temperature and rate of temperature change using energy conservation considerations [31].

An optimization method based on a direct and systematic search region reduction optimization method [32] can be employed to estimate the unknown convective heat transfer coefficient in a typical rocket nozzle. The most attractive feature of the direct search scheme is the simplicity of computer programming. The pseudo-random algorithm, an effective tool for optimization, does not require computation of derivatives but depends only on function evaluation. It works even when the differentiability requirements cannot be ensured in the feasible domain. For initiating the search only an estimate of the feasible domain is needed. Therefore, another advantage of the method is that the starting condition is not crucial; any reasonable value will do.

3. Heat conduction equation

3.1 Analytical solution

The computation of the turbulent convective heat transfer coefficient from combustion gases to the rocket nozzle wall is based on the Bartz's equation [33] incorporating the effects of compressibility, throat curvature and variation of transport properties in the boundary layer. The transient heat conduction in a one-dimensional Cartesian coordinate system having two parallel plane surfaces S_n (n = 1, 2) of a slab may be written in dimensional form [34] as.

$$\frac{\partial\theta(X,\tau)}{\partial\tau} = \frac{\partial}{\partial X}\left[K(\theta)\frac{\partial\theta(X,\tau)}{\partial X}\right], \text{in region } R, \tau>0 \tag{3}$$

with following initial and boundary conditions:

$$\theta(X,0) = f_i(X), \text{in region } R, \tag{4}$$

$$-\frac{\partial\theta(S_n,\tau)}{\partial X} = Bi_n[\theta(S_n,\tau)], \text{or } \frac{q_w L}{(T_g - T_i)} \text{ on boundary } S_n, \tau>0 \tag{5}$$

where f_i is initial temperature distribution in the region R of the slab. Eq. (4) represents both convective heat transfer or heat flux condition as applied to the inner surface.

We now consider the constant thermal property solution and can be written in terms of eigen function $\psi(\lambda_m, X)$ as

$$\theta(X,\tau) = \sum_{m=1}^{\infty} \exp\left[-\lambda_m^2\tau\right]\psi(\lambda_m, X)\int_R \psi(\lambda_m\overline{X})f(\overline{X})d\overline{X} \tag{6}$$

In the above Eq. (5), Bi or q_w is the unknown parameter to be determined using measured temperature time history at location x_m as depicted in **Figure 1**. In estimating the unknown condition, one has to minimize the absolute difference between the calculated and measured temperature at specified location and time (x_m, τ) in a prescribed tolerance value using an iteration procedure. The iteration scheme is described in the following sections.

3.2 Inverse algorithm

The IHCP is solved by comparing calculated and measured temperature using an iterative technique [30]. In estimating q_w, one minimizes

$$F(q_w) \approx |\theta_c(X_m, \tau) - \theta_m(X_m, \tau)| \tag{7}$$

where θ_c and θ_m are the calculated and measured temperatures at (X_m, τ), respectively. The computed temperature is a nonlinear function of unknown parameters such as wall heat flux or convective heat transfer coefficient. Temperature is calculated using Eq. (6) and compared with the measured temperature as expressed in Eq. (7). The inverse problem starts with initial guess value of the unknown parameter. The second step is to correct the previous guessed unknown parameter using the Newton-Raphson method. The sensitivity coefficient can be obtained by differentiating temperature with respect to wall heat flux q_w. The iteration procedure will continue until $|F(q_w)| \leq 10^{-4}$. This iterative scheme estimates the component of the q_w at a time and thus may be considered on-line method.

The inverse method for solving a value of $q_w(0, \tau)$ is as follows. Initiate with an initial guess value of q_w, satisfy the convergence criterion, and implement the Newton-Raphson to obtain the estimate value.

Now, it is possible to estimate convective heat transfer coefficient and combustion gas temperature in conjunction with measured temperature history [35]. The equation for converting the calculated heat flux to the heat transfer coefficient is

$$Bi = \frac{Lq_w}{K(\theta)(T_g - T_i)} \tag{8}$$

In the foregoing equation, T_g is an unknown quantity and can be estimated using again the above-mentioned minimization and iteration methods. The convergence criterion for the iterative scheme remains same as mentioned above.

3.3 Numerical methods

It is not always feasible to obtain analytical solution of temperature-dependent thermal conductivity and radiation boundary condition. The Crank-Nicolson finite difference method with two-time level implicit numerical scheme [36] has been employed to solve the nonlinear conduction problem with the Newton-Raphson method to consider the radiation boundary condition.

Deforming or moving finite elements method [37] is used to solve linear heat conduction equation. The moving finite element [38] is used to consider the time delay in the measurement of back wall temperature.

3.4 Two-nodes system of transient heat conduction equation

For only two nodes the system of [39] equations reduce to the following pair of equations:

$$\frac{d\theta_0}{d\tau} = \frac{1}{(\Delta X)^2}[-2(\theta_1 + Bi\Delta X)\theta_0 + 2\theta_1] \tag{9}$$

$$\frac{d\theta_1}{d\tau} = \frac{1}{(\Delta X)^2}[2\theta_0 - 2\theta_1] \tag{10}$$

where 0 and 1 represent node in a slab of finite thickness. These are the exact solutions to the system of two ordinary differential equations which resulted from a two-node finite-difference approximation to the original problem.

$$\theta_0 = \frac{1}{\lambda_2 - \lambda_1}\left[(\lambda_2 + 2Bi)e^{\lambda_1 \tau} - (\lambda_1 + 2Bi)e^{\lambda_2 \tau}\right] \tag{11}$$

$$\theta_1 = \frac{1}{\lambda_2 - \lambda_1}\left[\lambda_2 e^{\lambda_1 \tau} - \lambda_1 e^{\lambda_2 \tau}\right] \tag{12}$$

where $\lambda_1 = -2 - Bi + \sqrt{Bi^2 + 4}$ and $\lambda_2 = -2 - Bi - \sqrt{Bi^2 + 4}$.

Solution of the above simultaneous equation calculates the temperature with a given value of Bi. The solution is now solving simultaneously Eqs. (11) and (12) to determine the unknown parameter.

4. Inverse problem of heat conduction applied to a rocket nozzle

The influence of constant (average) thermal conductivity, temperature-dependent thermal conductivity, computational grid in numerical solver, nonlinear boundary condition, cylindrical coordinate and the estimation of the wall heat flux and convective heat transfer is carried out by employing measured temperature history of a rocket nozzle of a solid motor. Solution of linear heat conduction equation is used to estimate the convective heat transfer coefficient with the measured temperature data of outer wall of a rocket nozzle. The running time of rocket motor is 16 s. The nozzle wall thickness L = 0.0211 m. The thermo-physical properties of the material are: ρ = 7900 kg m^{-3}, C_p = 545 J kg^{-1} K^{-1}, K (average) = 35 Wm^{-1} K^{-1}. Initial temperature T_i = 300 K and combustion gas temperature T_g = 2946.2 K are used in the solution of the heat conduction equation.

4.1 Average thermal conductivity

Prediction of convective heat transfer coefficient is carried out in conjunction with the calculated and measured temperature history at outer surface of nozzle divergent in a solid rocket motor static test. The constant thermal conductivity solution of the linear transient heat conduction problem [30] is

$$\theta(X, \tau) = 1 - 2\sum_{n=1}^{\infty} \frac{Bi}{\left(Bi^2 + \lambda_n^1 + Bi\right)} \frac{\cos\left[\lambda_n(1 - X)\right]}{\cos \lambda_n} e^{-\lambda_n^2 \tau} \tag{13}$$

$$\lambda \tan \lambda = Bi \tag{14}$$

For estimating unknown boundary condition, the heat conduction equation is and solved with the following boundary and initial conditions.

$$\frac{\partial \theta(0, \tau)}{\partial X} = Bi[\theta(0, \tau) - 1], \tau > 0 \tag{15}$$

$$\frac{\partial \theta(1, \tau)}{\partial X} = 0, \tau > 0 \tag{16}$$

and

$$\theta(X, 0) = 0, \text{for all } X \tag{17}$$

Exact analytical solution of transient heat conduction as written in Eq. (13) is used to estimate convective heat transfer on the inner surface of the rocket nozzle.

An iterative scheme is used to solve inverse problem [30]. The iteration is carried out till the absolute difference between calculated and measured temperature is less than or equal to 10^{-4}. **Table 1** exhibits the comparison between the estimated values of the convective heat transfer coefficient based on the exact solution of heat conduction equation with the calculated values of Bartz [33]. Bartz's equation calculates conservative estimates for the convective heat transfer to the wall [40].

4.2 Temperature-dependent thermal conductivity

An iteration procedure [41] is employed in conjunction with exact solution to predict convective heat transfer coefficient from the measured temperature-time data at the outer wall of the nozzle as shown in **Table 2**. The expression for temperature-dependent conductivity is $K(T) = k_0 - \beta T$. The value of k_0 and β are 57 $Wm^{-1}\,K^{-1}$ and 2.718 $Wm^{-1}\,K^{-2}$, respectively. The advantage of using the exact solution is found directly at specified location and time as compared to the numerical method which needs the computation from the initial state.

4.3 Numerical solution with various computational grids

Deforming or moving finite element is used to consider the time delay in temperature at the outer wall of the slab [37]. Estimated values of wall heat flux and heat transfer coefficient are tabulated in **Table 3**. It can be observed from the table that the estimated wall quantities are having significant influence on the predicted unknown boundary conditions. This example is extended to consider spatial grid changed and temporal dependence on the numerical solution using moving finite element method [38].

4.4 Nonlinear boundary condition

Numerical analysis of nonlinear heat conduction with a radiation boundary condition [36] is carried out to estimate wall heat flux using temperature history on the back wall of the rocket nozzle. The high temperature variation alters thermophysical properties of the material of mild steel. **Table 4** shows comparison

t, s	θ_0 at inner surface	θ_c at outer surface	θ_m at outer surface	h, W/m^2K	h_B, W/m^2K
6	0.2950	0.0098	0.0096	1821.9	2254.2
7	0.3109	0.0159	0.0158	1810.0	2254.2
8	0.2996	0.0212	0.0211	1610.3	2254.2
9	0.3244	0.0301	0.0302	1690.9	2254.2
10	0.3340	0.0386	0.0385	1669.7	2254.2
11	0.3416	0.0473	0.0472	1641.9	2254.2
12	0.3302	0.0529	0.0529	1497.6	2254.2
13	0.3312	0.0602	0.0604	1443.1	2254.2
14	0.3409	0.0677	0.0676	1387.0	2254.2
15	0.3442	0.0781	0.0782	1413.0	2254.2
16	0.3475	0.0862	0.0861	1383.7	2254.2

Table 1.
Solution of inverse heat conduction problem.

t, s	$\theta(0, \tau)$				h, W/m^{2}K	
	Iterative method	Beck method	$\theta_c(1, \tau)$	$\theta_m(1, \tau)$	Iterative method	Beck method
6	0.0883	0.0838	0.0099	0.0098	536.6	581.7
7	0.1067	0.1075	0.0158	0.0159	600.6	587.0
8	0.1144	0.1116	0.0220	0.0212	592.6	598.4
9	0.1367	0.1367	0.0302	0.0302	674.2	685.3
10	0.1522	0.1545	0.0386	0.0385	712.9	693.2
11	0.1654	0.1690	0.0472	0.0472	737.4	730.0
12	0.1686	0.1639	0.0529	0.0529	718.2	721.9
13	0.1773	0.1777	0.0605	0.0605	723.6	725.8
14	0.1844	0.1813	0.0677	0.0676	723.0	725.1
15	0.1944	0.2040	0.0781	0.0782	753.6	765.0
16	0.2083	0.2174	0.0862	0.0862	758.3	770.0

Table 2.
Comparison between iterative and Beck methods.

t, s	T_m K at $X = 1$	Uniform grid		Non-uniform grid		Moving grid	
		$q_w \times 10^6$, W/m^2	h_c, W/m^{2}K	$q_w \times 10^6$, W/m^2	h_c, W/m^{2}K	$q_w \times 10^6$, W/m^2	h_c, W/m^{2}K
6	326	3.715	1964.5	3.846	2044.9	4.517	2412.1
7	342	2.700	1408.8	2.848	1449.6	2.818	1485.9
8	356	2.698	1436.9	2.840	1531.6	2.820	1512.8
9	380	2.704	1463.0	2.589	1569.8	2.842	1552.8
10	402	2.705	1491.4	2.858	1603.3	2.846	1586.7
11	425	2.704	1518.9	2.852	1632.6	2.845	1618.5
12	440	2.691	1539.7	2.805	1636.2	2.812	1630.8
13	460	2.683	1564.6	2.776	1649.7	2.791	1650.6
14	479	2.673	1588.1	2.738	1657.1	2.764	1665.9
15	507	2.094	1226.4	2.015	1190.6	2.091	1235.4
16	528	2.086	1231.8	1.981	1178.5	2.067	1231.6

Table 3.
Wall heat flux at various grid arrangements.

between the estimated convective heat transfer coefficients with the Bartz solution [33]. Effects of nonlinear IHCP with radiation boundary condition are investigated and results are presented in **Table 4**.

4.5 Heat conduction in a hollow cylinder

A grid point shift strategy [42] is adapted to solve inverse conduction problem in a radial coordinate of rocket nozzle with inner and outer radius of rocket nozzle. The inner and outer radius of the nozzle is 0.0839 m and 0.0105 m, respectively. The purpose of the present example to investigate the influence of radial coordinate

t, s	T_o, K at $X = 0$	T_m K at $X = 1$	$q_c \times 10^6$ W/m^2	h W/m^{2}K	h_B W/m^{2}K	T_{gc} K	T_g K
6	659.8	326	2.3547	950.0	2254.2	3137	2946.2
7	801.0	342	2.3899	1019.6	2254.2	3122	2946.2
8	900.7	356	2.2211	992.4	2254.2	3115	2946.2
9	996.3	380	2.6489	1237.1	2254.2	3113	2946.2
10	1050.5	402	2.3670	1135.5	2254.2	3108	2946.2
11	1066.4	425	1.7100	827.3	2254.2	3104	2946.2
12	1201.8	440	2.8144	1459.2	2254.2	3099	2946.2
13	1320.0	460	2.6559	1467.0	2254.2	3098	2946.2
14	1354.8	479	1.7595	991.7	2254.2	3095	2946.2
15	1383.4	507	1.3810	791.4	2254.2	3094	2946.2
16	1414.9	528	1.1684	681.8	2254.2	3094	2946.2

Table 4.
Solution with nonlinear boundary condition.

t, s	T_o K at $X = 0$	T_m K at $X = 1$	$q_c \times 10^6$ W/m^2	h, W/m^{2}K	h_B, W/m^{2}K	θ_g, K	θ_{gc}, K
6	1260.2	326	3.6805	1789.6	2254.2	3316	2946
7	1175.9	342	3.3995	1628.0	2254.2	3264	2946
8	1160.7	356	2.4745	1181.4	2254.2	3255	2946
9	1165.8	380	2.5385	1194.7	2254.2	3290	2946
10	1196.0	402	2.5348	1261.1	2254.2	3206	2946
11	1192.3	425	2.3385	1166.4	2254.2	3197	2946
12	1205.8	440	2.2094	1114.8	2254.2	3187	2946
13	1211.0	460	2.1333	1229.5	2254.2	2946	2946
14	1222.1	479	2.0441	1187.5	2254.2	3943	2946
15	1237.1	507	2.0626	1206.7	2254.2	2946	2946
16	1249.1	528	2.0027	1180.9	2254.2	2945	2946

Table 5.
Inverse problem in a hollow cylinder.

on the estimated values of heat transfer coefficient. **Table 5** shows the effect of geometrical parameters on the predicted heat transfer coefficient.

4.6 Estimation of heat flux and heat transfer coefficient

The calculated convective heat transfer coefficients and inner wall temperature are used to determine the wall heat flux and the combustion temperature using Eq. (8). The iterative scheme is based on relation between wall heat flux and convective heat transfer coefficient [35]. **Table 6** shows the predicted values of wall heat flux and convective heat transfer coefficient. The IHCP is extended to determine wall heat flux in conjunction with convective heat transfer coefficient. A similar IHCP but referring to the 122 mm medium-range missile during correction engine operation has been considered by Zmywaczyk et al. [43].

t, s	T_0 K at $X = 0$	T_m K at $X = 1$	$q_c \times 10^6$, W/m^2	h, W/m^{2}K	h_B, W/m^{2}K	T_g, K	T_{gc}, K
6	1355.6	326	3.2502	2631.2	2254.2	3351	2946
7	1287.8	342	3.2950	1805.3	2254.2	3113	2946
8	1315.6	356	3.2974	1861.5	2254.2	3087	2946
9	1368.9	380	3.2967	1885.9	2254.2	3117	2946
10	1414.4	402	3.2837	1962.1	2254.2	3088	2946
11	1463.6	425	3.2718	2049.5	2254.2	3060	2946
12	1370.8	440	2.3825	1476.0	2254.2	2985	2946
13	1360.9	460	2.4140	1502.1	2254.2	2968	2946
14	1370.3	479	2.3625	1520.6	2254.2	2924	2946
15	1382.5	507	2.3675	1517.2	2254.2	2943	2946
16	1399.3	528	2.3645	1540.7	2254.2	2934	2946

Table 6.
Wall heat flux and convective heat transfer coefficient.

5. Estimation of heat flux with two-nodes in a sounding rocket

A two-node exact solution is used to calculate the back-wall temperature as described in Section 3.4. The iterative method described above has been used for estimating aerodynamic heating for a sounding rocket in free flight test. Here, the wall heat flux is estimated using the measured temperature history in conjunction with the iterative technique [30]. The aerodynamic heating rate is estimated for a typical sounding rocket as depicted in **Figure 2**. The location of thermocouple is marked in the diagram. The thermophysical properties of Inconel and wall thickness are $k = 18$ Wm^{-1} K^{-1}, $\alpha = 4.47 \times 10^{-6}$ m^2/s, $L = 0.7874 \times 10^{-3}$ m. **Figure 3** depicts the measured temperature time history at different locations measured from the tip of the cone in the free flight of a sounding rocket as delineated in **Figure 2**. It can be observed from temperature history that the initial time delay in thermal response is 6 s. The unknown q_w are estimated using an iterative technique which starts with an initial value of wall heat flux and is repeated until $|F(q_w)| \leq 10^{-4}$.

A two-node exact solution is used to calculate the wall temperature distribution. The unknown q_w are estimated using an iterative technique which starts with an initial value of wall heat flux and is repeated until $|F(q_w)| \leq 10^{-4}$. **Figure 4** displays the estimated variation of the wall heat flux as a function of flight time of the sounding rocket.

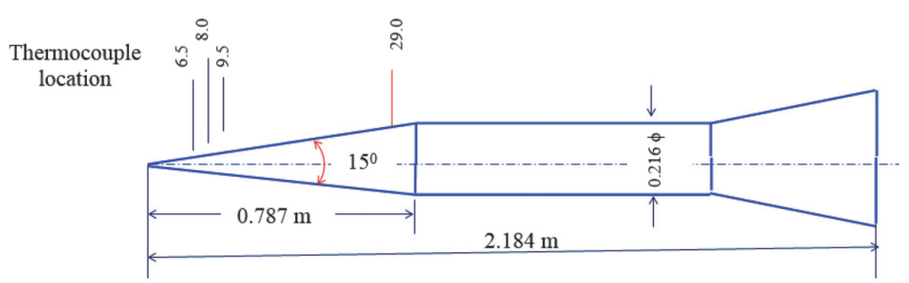

Figure 2.
Schematic sketch of sounding rocket showing location of thermocouple.

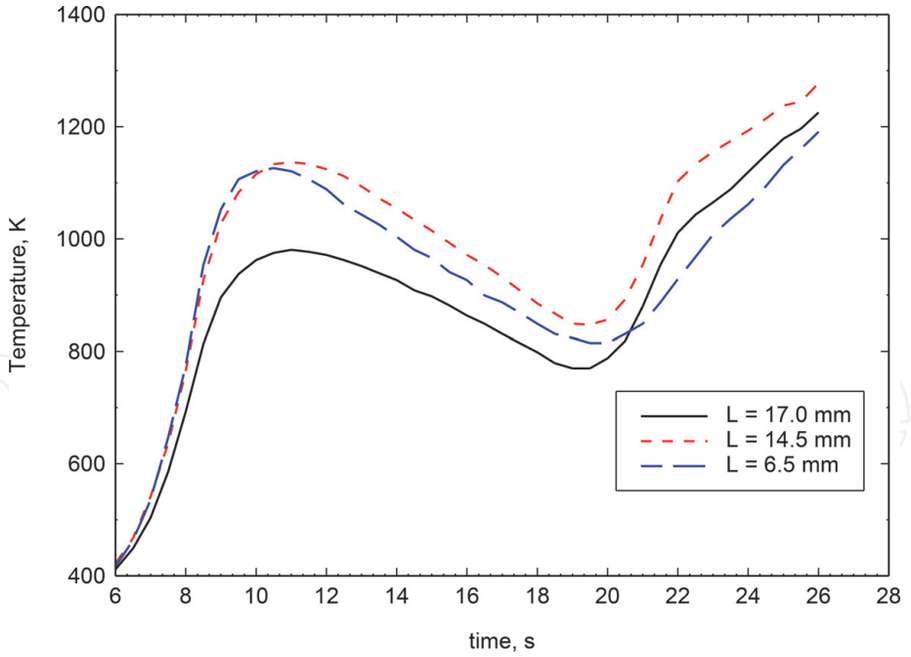

Figure 3.
Measured temperature history in free flight of the sounding rocket.

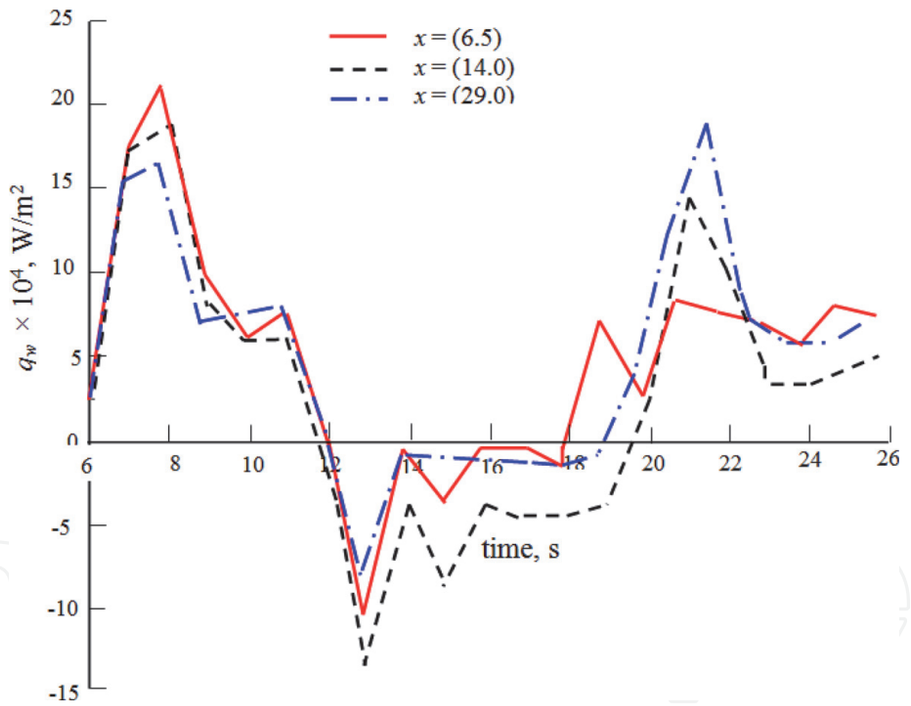

Figure 4.
Variations of wall heat flux vs. flight time.

The wall heat flux variation depends on the sounding rocket speed. The increase and decrease of the aerodynamic heating are a function of flight Mach number.

The estimated wall heat flux is compared with Van Driest's results [44]. **Table 7** depicts the estimated values of wall heat flux as a function of flight time at thermocouple location 29 as shown in **Figure 2**. It can be observed from the table that highest aerodynamic heating occurs during 7–8 s, another significant peak wall heat flux was found at 22 s.

t, s	T_m, K	T_c, K	$q_w \times 10^4$, W/m^2	$q_w^{\text{van}} \times 10^4$, W/m^2
6	313.0	320.0	2.756	8.246
7	341.3	349.4	16.695	14.82
8	408.0	412.3	19.387	22.647
9	469.7	469.3	8.657	18.876
10	495.2	495.8	8.145	10.117
11	504.1	513.3	9.302	4.569
12	502.4	521.2	2.757	1.176
13	495.2	506.8	−7.695	−0.977
14	487.4	487.6	−0.040	−2.320
15	477.4	477.0	−0.037	−3.134
16	467.4	467.0	−0.028	−3.578
17	457.4	457.5	−0,034	−3.769
18	445.8	447.2	−0.905	−3.789
19	438.6	437.5	−0,005	−1.628
20	444.1	445.9	5.173	4.135
21	469.1	467.5	13.518	11.524
22	533.0	521.2	20.618	19.732
23	556.3	558.4	9.180	13.122
24	567.1	573.5	6.514	8.581
25	584.1	587.2	8.592	5.467
26	596.9	602.2	7.018	3.314

Table 7.
Comparison between calculated and Van Driest's heat flux at location 29.

6. Conclusions

Analytical, transient numerical and two-node methods are used to compute temperature distribution in a finite slab. Numerical solution is carried out with temperature-dependent thermal conductivity. Implicit finite difference scheme with two-time level technique is implemented to solve nonlinear problem of heat conduction. Time delay is studied using finite element method with deforming grid strategy. A boundary shifting numerical scheme is used to solve transient heat conduction in radial coordinate. Evidence of temporal accuracy and dependence on time-step is demonstrated in the numerical solving of IHCP. Influence of thermocouple cavity and measurement errors in location and time are discussed. The IHCP is applied to predict the wall heat flux in a rocket nozzle of a solid motor. Wall heat flux is estimated in a free flight of a sounding rocket using the two-node method.

Nomenclature

Bi	Biot number, hL/k
C_p	specific heat
h	heat transfer coefficient
$K(\theta)$	thermal conductivity, $k(\theta)/k_0$

k_0	reference thermal conductivity at T_i
L	slab thickness
p	nondimensional parameter, $\alpha\Delta T/(\Delta x)^2$
q_w	wall heat flux
T	temperature
t	time
x	distance from the inner surface
X	dimensionless coordinate
α	thermal diffusivity
ρ	density
θ	nondimensional temperature, = $(T - T_g)/(T_g - T_i)$
τ	nondimensional time, $\alpha t/L^2$

Subscripts

B	Bartz
c	computed
g	combustion gas temperature
i	initial value
m	measured
o	outer wall
w	wall
β	constant thermal conductivity coefficient

Author details

Rakhab C. Mehta
Department of Aeronautical Engineering, Noorul Islam Centre for Higher Education, India

*Address all correspondence to: drrakhab.mehta@gmail.com

References

[1] Stolz G. Numerical solutions to an inverse problem of heat conduction for simple shapes. Journal of Heat Transfer. 1960;**82**(1):20-26

[2] Burggraf OR. An exact solution of the inverse problem in heat conduction theory and applications. Journal of Heat Transfer. 1964;**86**(2):373-382

[3] Beck JV. Nonlinear estimation applied to the nonlinear heat conduction problem. International Journal of Heat and Mass Transfer. 1970;**13**:703-716

[4] Frank I. An application of least squares method to the solution of the inverse problems of heat conduction. Journal of Heat Transfer. 1963;**85**: 378-379

[5] Imber M, Kan J. Prediction of transient temperature distributions with embedded thermocouples. AIAA Journal. 1972;**10**:784-789

[6] Shumakov NV. A method for the experimental study of the process heating a solid body. Journal of Technical Physics of the Academic of Sciences USSR. 1957;**2**:771-777

[7] Vogel J, Sára L, Krejčí L. A simple inverse heat conduction method with optimization. International Journal of Heat and Mass Transfer. 1993;**36**(17): 4215-4220

[8] Beck JV, Blackwell B, St. Clair CR Jr. Inverse Heat Conduction, Ill-Posed Problems. New York: Wiley-Interscience Publication; 1977

[9] Özisik MN, Orlande HRB. Inverse Heat Transfer: Fundamentals and Applications. New York: Taylor and Francis; 2000

[10] Tikhonov AN, Arsenin VY. Solution of Ill-Posed Problems. Washington, DC: Winston & Sons; 1977

[11] Kurpisz K, Nowak AJ. Inverse Thermal Problems. Southampton, UK: Computational Methods Publications; 1995

[12] Hensel E. Inverse Theory and Applications for Engineers. New Jersey: Prentice Hall; 1991

[13] Alifanov OM. Inverse Heat Transfer Problems. Berlin, Germany: Springer-Verlag; 1994

[14] Taler J, Duda P. Solving Direct and Inverse Heat Conduction Problems. Berlin: Springer; 2006

[15] Rumsey CB, Lee DB. Measurements of aerodynamic heat transfer on a 15-degree cone-cylinder, flare configuration in free-flight at Mach numbers up to 4.7. NASA TN D-824; 1961

[16] Mehta RC. Estimation of aerodynamic heat transfer in free-flight at Mach number upto 4.7. Wärm-und Stüffubertrang. 1986;**20**:27-31

[17] Mehta RC, Jayachandran T, Sastri VMK. Finite element analysis of conduction and radiative heating of a thin skin calorimeter. Wärm-und Stüffubertrang. 1988;**22**:227-230

[18] Dąbrowski A, Dąbrowski L. Inverse heat transfer problem solution of sounding rocket using moving window optimization. PLoS One. 2019;**14**(6):1-24

[19] Howard FG. Single thermocouple method for determining heat flux to a thermally thick wall. NASA TN D 4737; 1968

[20] Zmywaczyk J, Koniorczyk P. Numerical solution of inverse radiative-conductive transient heat transfer problem in a grey participating medium. International Journal of Thermophysics. 2009;**30**:1438-1451

[21] Karnal M. High temperature measurements at the internal nozzle wall of the zephyr [MS thesis]. Germany: Department of Computer Science, Electrical and Space Engineering, Lulea University of Technology; 2014

[22] Heisler MP. Temperature charts for induction and constant temperature heating. Journal of Heat Transfer, Transactions of the ASME. 1947;**69**: 227-236

[23] Mehta RC, Jayachandran T. Determination of heat transfer coefficient using transient temperature response chart. Wärm-und Stüffubertrang. 1990;**26**:1-5

[24] Li DI, Wells MA. Effects of subsurface thermocouple installation on the discrepancy of the measured thermal history and predicted surface heat flux during a quench operation. Metallurgical and Materials Transactions B. 2005;**36**(3):343-354

[25] Perakis N, Haidin OJ. Inverse heat transfer method applied to capacitively cooled rocket thrust chambers. International Journal of Heat and Mass Transfer. 2018;**131**:150-166

[26] Woodbury KA. Effect of thermocouple sensor dynamics on surface heat flux prediction obtained via inverse heat conduction analysis. International Journal of Heat and Mass Transfer. 1990;**33**(12):2641-2649

[27] Chen CJ, Danh TM. Transient temperature distortion in a slab to thermocouple cavity. AIAA Journal. 1978;**14**(7):979-981

[28] Anil SL, Mehta RC. Effect of thermocouple cavities on heat transfer measurements. In: Proceedings of XVII National and VI ISHMT/ASME Heat and Mass Transfer Conference, HMT-2004-C68, IGCAR, Kalpakam, India. Jan. 2004

[29] Carslaw HD, Jaeger JC. Conduction of Heat in Solids. London, UK: Oxford University Press; 1959

[30] Mehta RC. Solution of the inverse conduction problem. AIAA Journal. 1977;**15**(9):1355-1358

[31] Mehta RC. Estimation of heating rate using a calorimeter probe. Review of Scientific Instrumentation. 1987; **52**(11):1782-1784

[32] Mehta RC, Tiwari SB. Controlled random search technique for estimation of convective heat transfer coefficient. Heat and Mass Transfer Journal. 2007; **43**:1171-1177

[33] Bartz DR. A simple equation for rapid estimation of rocket nozzle convective heat transfer coefficients. Jet Propulsion. 1957;**27**:49-51

[34] Özisik MN. Boundary Value Problem of Heat Conduction. USA: International Text Book Co; 1968

[35] Mehta RC. Estimation of heat transfer coefficient in a rocket nozzle. AIAA Journal. 1981;**19**(8): 1085-1086

[36] Mehta RC. Numerical solution of nonlinear inverse heat conduction problem with radiation boundary conditions. International Journal of Numerical Methods in Engineering. 1984;**20**:1057-1066

[37] Mehta RC, Jayachandran T. Deforming finite element for the numerical solution of the nonlinear inverse heat conduction problem. Communication in Applied Numerical Methods. 1987;**3**:167-172

[38] Mehta RC, Jayachandran T. Deforming grid method applied to the inverse problem of heat conduction. Journal of Thermophysics and Heat Transfer. 1989;**3**(2):226-229

[39] Myers GF. Analytical Method in Conduction Heat Transfer. New York, USA: McGraw-Hill; 1971

[40] Brinsmade AF, Desmon LG. Hypothesis for correlating rocket nozzle throat convective heat transfer. Heat Transfer-Cleveland, Chemical Engineering Progress Symposium. 1965; **61**(59):88-98

[41] Mehta RC. Extension of the solution of inverse conduction problem. International Journal of Heat and Mass Transfer. 1979;**22**:1149-1150

[42] Mehta RC. An efficient numerical method for solving inverse conduction problem in a hollow cylinder. AIAA Journal. 1984;**22**(6):860-862

[43] Zmywaczyk J, Koniorczyk P, Preiskorn M, Machowski B. An inverse approach to estimate heat transfer coefficients of 122 mm medium-range missile during correction engine operation, problems of mechatronics armament, aviation. Safety Engineering. 2014;**5**(15):25-40

[44] Van Driest ER. In: Lin CC, editor. Turbulent Flows and Heat Transfer, 6. Princeton, NJ, USA: Princeton University Press; 1959